https://doi.org/10.17221/84/2024-SWR

Fractal parameters of soil particle size distribution in karst area, and implications of soil water repellency by plantations

Zhuo Tian[1,2], Haitao Deng[2,3], Shuaipu Zhang[2,3], Qinxue Xu[2,3], Xin Jin[2,3]*

[1]*College of Agricultural Science and Engineering, Hohai University, Nanjing, Jiangsu, P.R. China*
[2]*Guangxi Key Laboratory of Environmental Pollution Control Theory and Technology, Guilin University of Technology, Guilin, Guangxi, P.R. China*
[3]*Engineering Research Center of Watershed Protection and Green Development, University of Guangxi, Guilin University of Technology, Guilin, Guangxi, P.R. China*

**Corresponding author: shuaipuzhang@glut.edu.cn*

Citation: Tian Z., Deng H.T., Zhang S.P., Xu Q.X., Jin X. (2025): Fractal parameters of soil particle size distribution in karst area, and implications of soil water repellency by plantations. Soil & Water Res., 20: 93–104.

Abstract: As a critical and universal soil physical property, soil water repellency significantly affects soil and water erosion and vegetation restoration, particularly in the karst region. This study analysed soil properties, namely, particle size distribution (PSD) in abandoned farmland and different plantations in karst areas, and their impact on water repellency to provide references for its ecological restoration. First, for the shaddock plantation, citrus plantation, ginkgo plantation, *Robinia pseudoacacia* plantation, and abandoned farmland, the research objects, soil particle size and water drop penetration time were measured, and the fractal parameters of soil PSD were computed. Soil PSD characteristics' influence on water repellency was inferred according to, for example, correlation, redundancy, and stepwise regression analyses. Sand content in the shaddock plantation and clay content in the citrus plantation was the highest. The soil particles of abandoned farmland and plantations were primarily sand. The values of volume dimension $D(0)$ in descending order were citrus plantation, shaddock plantation, ginkgo plantation, *R. pseudoacacia* plantation, and abandoned farmland. The values of information dimension $D(1)$, correlation dimension $D(2)$, and information dimension/volume dimension $D(1)/D(0)$ in descending order were *R. pseudoacacia* plantation, ginkgo plantation, citrus plantation, abandoned farmland, and shaddock plantation. No significant differences were found in the symmetry degree Δf, the spectral width $\Delta\alpha$ of the singular spectral function, and the single fractal dimension D among the abandoned farmland and different plantations. Slight water repellency was observed in the abandoned farmland and different plantations. The degree of water repellency in descending order was *R. pseudoacacia* plantation > ginkgo plantation > abandoned farmland > citrus plantation > shaddock plantation. Significant correlations were found between fractal parameters and water repellency, and fractal parameters were suitable potential indicators for soil water repellency.

Keywords: multifractal; single fractal; soil particle size; water repellency

In karst areas, because the soil layer depth is low, it is easily erodible, with low land-bearing capacity, and the vegetation is vulnerable to disturbances due to the fragile ecological environment, making forest restoration challenging (Tian et al. 2016; Deng et al. 2020). As crucial components of forest ecosystems, plantations play a crucial role in increasing forest resources, as well as preventing soil erosion (Xu

Supported by the National Natural Science Foundation of China, Project No. 42267045, and Guangxi Science and Technology Program, Project No. AB21075007.

https://doi.org/10.17221/84/2024-SWR

et al. 2009; Duan et al. 2010; Banfield et al. 2018). The growth of plantations has become an important measure for improving soil quality and promoting the development of the ecological environment in karst areas (Pang et al. 2018; Yi et al. 2021). Soil is the foundation for vegetation survival, and differences in soil water repellency can cause an imbalance distribution of soil water, leading to uneven deformation of the soil, increasing surface runoff, and exacerbating soil erosion (Nunes et al. 2016; Vogelmann et al. 2017; Chen et al. 2020). Notably, studying soil water repellency characteristics of plantations in karst areas would deepen the understanding of infiltration and spatial variation in soil water and has reference significance for the prevention of soil erosion and the study of forest restoration (Roper et al. 2013; Abou Najm et al. 2021).

As a vital and universal soil physical property, soil water repellency can lead to water infiltration times ranging from seconds to days and reflects the soil's affinity for water (Doerr & Thomas 2000; Doerr et al. 2000; Buczko et al. 2005; Jordan et al. 2013). Soil is a porous medium with an irregular shape and self-similar structure, consisting of solid particles in various sizes and textures, shaped structurally by pores in different diameters and shapes (Carter 2004; Tian et al. 2023). The size of soil particles and their distribution characteristics can significantly affect the degree of soil water repellency (Sun et al. 2014). Studies have shown that soil water repellency varies by soil particle size (Qin et al. 2012; Sun et al. 2014). Fine-grained soil has a larger specific surface area and thus stronger adsorption capacity for water-repellent substances and stronger water repellency than coarse-grained soil (Zhang et al. 2013). Applying fractal theory is effective in studying soil particle size distribution (PSD) (Li et al. 2022). Single fractal theory can reveal the overall properties of soil PSD and capture its texture (Wang et al. 2022b). Multifractal theory can explain the PSD range of soil, provide local heterogeneity data on soil PSD, and evaluate the characteristics of the soil structure (Wang et al. 2022a). Exploring the correlation between soil PSD properties and water repellency by using single fractal and multifractal theories is of substantial importance for understanding slope runoff, sediment production, soil formation, and evolution processes.

The shallow depth of the soil layer in karst areas exhibits poor continuity (Deng et al. 2020). As a key factor in soil water holding and permeability, water repellency can regulate soil moisture and vegetation distribution in an area by influencing the hydrological processes at the surface and underground, which is crucial for local ecological restoration (Chen et al. 2020; Smettem et al. 2021). Notably, soil PSD and water repellency in karst areas and the influence mechanism of soil PSD on water repellency are poorly understood. Therefore, this study combined single fractal and multifractal theories to explore the soil PSD properties of shaddock plantation, citrus plantation, ginkgo plantation, *Robinia pseudoacacia* plantation, and abandoned farmland in karst areas and their impact on water repellency. The outcomes of this research are a useful source of data and support for further research on soil water infiltration, evaporation, and runoff. The outcomes also provide basic data and theoretical support for the simulation of ecological hydrological cycles in karst regions.

MATERIAL AND METHODS

Study area

The study area was in Futian village, Guilin City, Guangxi, China (110°29'30''–110°29'50''E, 25°4'40''–25°4'50''N; elevation of 280–330 m) and characterised by typical karstic peaks cluster landforms. Plantations were widely distributed, mainly consisting of shaddock plantation, citrus plantation, ginkgo plantation, and *R. pseudoacacia* plantation. The climate was subtropical monsoon, with hot weather and high humidity with frequent rainfall. The average annual temperature was 18.7 °C, with minimum and maximum temperatures from January to February and June to September, respectively. The average annual rainfall was 1 785.2 mm: highest in June and lowest in October.

Sample collection and laboratory analyses

In the study area, shaddock plantation, citrus plantation, ginkgo plantation, *R. pseudoacacia* plantation, and abandoned farmland were selected as research objects. The soil types were classified as Leptosols according to the World Reference Base for Soil Resources. Three standard plots (5 × 5 m) were designated in the abandoned farmland and different plantations, and there were three sampling points (1 × 1 m) for each standard plot. Further information is presented in Table 1. The sites were sampled during December 2022 on days without rain. After removing litter and humus layers from the soil surface, the samples were collected from the 0–20 cm

https://doi.org/10.17221/84/2024-SWR

soil layer. A total of three replicates were collected from each sampling point. The soil samples were then stored in polythene bags and air-dried at room temperature. Impurities such as gravel were eliminated, and then the soil was gently ground using a ceramic mortar and pestle (Li et al. 2022). Finally, the remaining soil was screened using a sieve (2 mm mesh) and stored in labelled Ziplock bags at room temperature (Li et al. 2022).

A soil sample weighing 0.5 g was placed in a 500 mL beaker, and 30% H_2O_2 (10 mL) was added over 24 h to remove organic matter. Subsequently, 10% HCl (5 mL) was added for 10 min to eliminate calcium carbonate. Residual H_2O_2 and HCl were thoroughly rinsed with ultrapure water. Next, the beaker was refilled with ultrapure water and left undisturbed for 12 h to allow for settling, after which the supernatant was discarded, and 0.05 mol/L NaOH (10 mL) was introduced. The particle sizes of the soil samples were measured using a laser particle size analyser (Mastersizer 3000, Malvern Panalytical, UK) (Tian et al. 2023). The wet sample dispersion unit (Hydro LV) was used. The Mie theory was applied, and the measurement obscuration was between 10–20%. The refractive index was 1.52, and the absorption coefficient was 0. The ultrapure water was used as a dispersant, and ultrasound was used for two minutes. In addition, the agitator speed was 2 500 r/min, and each sample was tested three times. The percentage volume of soil PSD was analysed for the range of 0.02–2 000 μm and was classified as clay (0–2 μm), silt (2–20 μm), and sand (20–2 000 μm) (Tian et al. 2023).

Soil water repellency was measured using the water drop penetration time (WDPT). A single droplet of ultrapure water (50 μL) was placed on the soil surface by using a burette from a height of approximately 10 mm to minimise any disturbances due to the impact of the water droplet, and infiltration was timed with a stopwatch. Each sample was tested six times. The WDPT was classified as no water repellency (< 5 s), slight water repellency (5–60 s), strong water repellency (60–600 s), severe water repellency (600–3 600 s), or extreme water repellency (> 3 600 s) (Piyaruwan & Leelamanie 2020).

In addition, the collected soil samples were measured for total nitrogen (TN), electrical conductivity (EC), and pH with a Kjeldahl Distillation Unit (K9840, Hanon, China), an Electrical Conductivity Meter (DDS-307A, INESA, China), and a pH Meter (PHS-3E, INESA, China), respectively. Soil organic carbon (SOC) was determined by the potassium dichromate achromatic method. Soil organic matter (SOM) was measured via the dichromate oxidation method, and soil calcium carbonate ($CaCO_3$) was determined using the titration method. The basic physicochemical properties of the examined soils are listed in Table 2.

Calculation of fractal parameters

Single fractal dimension. The single fractal dimension D of soil PSD is calculated as follows (Bai et al. 2020):

$$\lg\left[\frac{V(r<R)}{V_T}\right]=(3-D)\times\left[\lg\left(\frac{R}{R_{max}}\right)\right] \quad (1)$$

where:

r – the particle size of the soil (μm);

R – a soil particle size of some grade (μm);

$V(r < R)$ – the summation volume of particle sizes less than R (%);

V_T – the total volume of soil particles (%);

R_{max} – the maximum soil particle size (μm).

Table 1. Basic information of sample plot

Sample plot	Latitude and longitude	Altitude (m)	Slope (°)	Stand density (plants/m^2)	Average tree height (m)	Average diameter at breast height (cm)
Shaddock plantation	110°29'42"E, 25°4'48"N	301.39	14.08	0.09	4.03	16.25
Citrus plantation	110°29'40"E, 25°4'47"N	319.12	27.33	0.18	2.61	1.81
Ginkgo plantation	110°29'49"E, 25°4'48"N	296.04	8.17	0.17	10.94	15.14
Robinia pseudoacacia plantation	110°29'44"E, 25°4'49"N	290.28	6.05	0.13	5.27	11.17
Abandoned farmland	110°29'49"E, 25°4'46"N	284.91	10.89	–	–	–

https://doi.org/10.17221/84/2024-SWR

Table 2. Soil basic physicochemical properties of sample plot

Sample plot	pH	Soil organic matter (g/kg)	Electrical conductivity (μs/cm)	Calcium carbonate	Soil organic carbon	Total nitrogen	Soil texture
				(g/kg)			
Shaddock plantation	5.21 ± 0.14^{ab}	23.67 ± 1.62^{ab}	241.02 ± 12.49^{b}	20.31 ± 0.70^{a}	13.73 ± 0.94^{ab}	1.92 ± 0.03^{a}	loamy sand
Citrus plantation	4.91 ± 0.10^{c}	25.43 ± 0.21^{a}	298.79 ± 29.98^{a}	20.24 ± 1.51^{a}	14.75 ± 0.12^{a}	2.07 ± 0.14^{a}	sandy clay loam
Ginkgo plantation	5.45 ± 0.10^{a}	22.26 ± 0.54^{b}	167.61 ± 13.74^{c}	18.69 ± 0.70^{ab}	12.91 ± 0.31^{b}	1.03 ± 0.16^{b}	sandy loam
Robinia pseudoacacia plantation	5.37 ± 0.11^{a}	25.19 ± 0.52^{a}	182.26 ± 5.86^{c}	18.10 ± 0.41^{b}	14.61 ± 0.30^{a}	1.05 ± 0.11^{b}	sandy loam
Abandoned farmland	4.99 ± 0.14^{bc}	25.24 ± 0.63^{a}	180.73 ± 8.57^{c}	17.53 ± 0.79^{b}	14.64 ± 0.37^{a}	1.95 ± 0.10^{a}	loamy sand

Values are mean ± standard deviation; the different lowercase letters in the same column indicated significant differences for the same variable between abandoned farmland and different plantations ($P < 0.05$)

Multifractal dimension. The measured interval $I = [0.02, 2000]$ (μm) was allocated to 64 cell intervals: $I_i = [\Phi_i, \Phi_{i+1}]$, $i = 1, 2, \ldots, 64$, with $\lg(\Phi_i / \Phi_{i+1})$ as a constant. A dimensionless interval $J = [0, 5]$ was constructed using the logarithmic transformation of the interval, calculated as follows (Gao et al. 2021):

$$\phi_i = \lg\left(\frac{\Phi_i}{\Phi_1}\right),\ i = 1, 2, \ldots, 65 \tag{2}$$

where:
ϕ_i – a dimensionless value of the equal interval;
Φ_i – the soil particle size (μm);
$\Phi_1 = 0.02$ μm.

In interval J, subintervals were computed in equal sizes as $N(\varepsilon) = 2^k$, where $\varepsilon = 5 \times 2^{-k}$ for k ranged from 1 to 6. $N(\varepsilon)$ is the subinterval number, and ε is the length of the step (Ke et al. 2021).

$\mu_i(\varepsilon)$ is identified as the possibility of finding particles of a given soil mass within the particle size interval J_i. The generalised fractal dimension $D(q)$ is determined as follows (Tian et al. 2023):

$$D(q) = \lim_{\varepsilon \to 0} \frac{1}{q-1} \frac{\lg\left[\sum_{i=1}^{N(\varepsilon)} \mu_i(\varepsilon)^q\right]}{\lg\varepsilon} (q \neq 1) \tag{3}$$

$$D(1) = \lim_{\varepsilon \to 0} \frac{\sum_{i=1}^{N(\varepsilon)} \mu_i(\varepsilon) \lg \mu_i(\varepsilon)}{\lg\varepsilon} (q = 1) \tag{4}$$

where:
$D(0)$ – the volume dimension;
$D(1)$ – the information dimension;
$D(2)$ – the correlation dimension;
q – the probability density weight index, which in this study is an integer in [–10, 10].

The multifractal singularity index $\alpha(q)$ and spectrum function $f[\alpha(q)]$ of the soil PSD are calculated as follows (Tian et al. 2023):

$$\alpha(q) = \lim_{\varepsilon \to 0} \frac{\sum_{i=1}^{N(\varepsilon)} \mu_i(q,\varepsilon) \lg \mu_i(\varepsilon)}{\lg\varepsilon} \tag{5}$$

$$f(\alpha(q)) = \lim_{\varepsilon \to 0} \frac{\sum_{i=1}^{N(\varepsilon)} \mu_i(q,\varepsilon) \lg \mu_i(q,\varepsilon)}{\lg\varepsilon} \tag{6}$$

where $\mu_i(q,\varepsilon)$ is defined as follows(Tian et al. 2023):

$$\mu_i(q,\varepsilon) = \frac{\mu_i(\varepsilon)^q}{\sum_{i=1}^{N(\varepsilon)} \mu_i(\varepsilon)^q} \tag{7}$$

The spectral width and symmetry degree of the singular spectral function are calculated as follows (Wang et al. 2015):

$$\Delta\alpha = \alpha(q)_{\max} - \alpha(q)_{\min} \tag{8}$$

$$\Delta f = f[\alpha(q)_{\min}] - f[\alpha(q)_{\max}] \tag{9}$$

where:
$\Delta\alpha$ – spectral width;
Δf – symmetry degree;
$\alpha(q)_{\min}$ – the minimum value of $\alpha(q)$;
$\alpha(q)_{\max}$ – the maximum value of $\alpha(q)$.

https://doi.org/10.17221/84/2024-SWR

Statistical analysis

Fractal parameters were computed using MATLAB 2018 (MathWorks, Natick, Massachusetts, USA). Stepwise regression analysis and one-way analysis of variance (ANOVA) were conducted using SPSS Ver. 22.0 (IBM Corporation, Armonk, New York, USA). Redundancy analysis was performed using Canoco Ver. 5.0 (Microcomputer Power, Ithaca, New York, USA). Pearson's correlation analysis and figure plotting were performed using Origin Pro 2021 (OriginLab, Northampton, Massachusetts, USA).

RESULTS

Soil PSD. The frequency curves of soil PSD denoted that the abandoned farmland and different plantations had soils with distinct compositional characteristics (Figure 1A). The soil texture in citrus plantation was finer than in shaddock plantation. The soil particles of abandoned farmland and different plantations were primarily sand, and the differences were noticeable (Figure 1B). The average sand content of shaddock plantation, citrus plantation, ginkgo plantation, *Robinia pseudoacacia* plantation, and abandoned farmland was 87.35%, 64.82%, 70.57%, 76.45%, and 85.62%, respectively, and the average clay content was 6.43%, 20.20%, 11.98%, 0.12%, and 0.23%, respectively. The sand content in citrus plantation, ginkgo plantation, and *R. pseudoacacia* plantation decreased by 24.29%, 17.58%, and 10.71%, respectively, compared with that in abandoned farmland, and increased by 2.02% in shaddock plantation. Furthermore, the clay content of plantations significantly increased compared with that of the abandoned farmland, with an increase ranging from 2695.65% to 8682.61%, except for in *R. pseudoacacia* plantation.

Fractal characteristics of soil PSD. The generalised dimensional spectral curves demonstrated a converse S-shaped declining function as the q value enlarged. When $q > 0$, the decrease in $D(q)$ was small and gradually levelled off (Figure 2A). When $q < 0$, the change in $D(q)$ was large and was, in descending order, ginkgo plantation > citrus plantation > *R. pseudoacacia* plantation > shaddock plantation > abandoned farmland, indicating that the fineness of the soil fractal structure in plantations was higher than that in the abandoned farmland. When $q > 0$, the variation amplitude of $D(q)$ was used to represent the uniformity level of soil PSD. The lesser the variation amplitude, the higher uniform the PSD. In this study, the order of uniformity of soil PSD was *R. pseudoacacia* plantation > ginkgo plantation > abandoned farmland > citrus plantation > shaddock plantation. The singular spectral curves of the soil in the abandoned farmland and the different plantations were asymmetric, convex-up, and left-deviating unimodal functions (Figure 2B). This outcome demonstrated that soil PSD exhibits non-uniform characteristics, and the soil particles with a sizeable volume fraction play a dominant role in the variability of soil PSD.

Abandoned farmland and different plantations presented a higher volume dimension $D(0)$ than

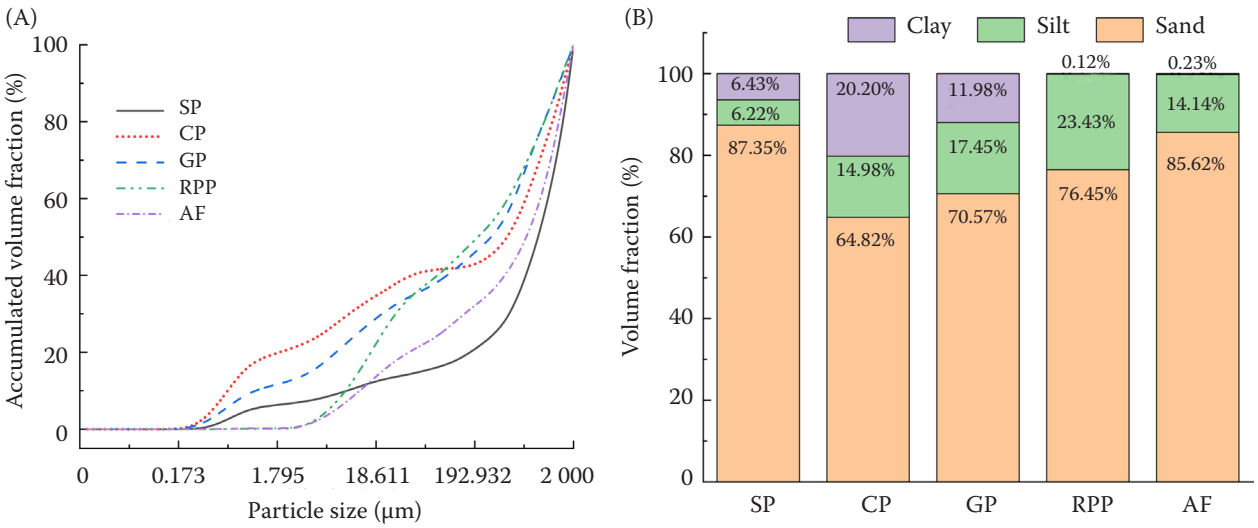

Figure 1. Soil particle size distribution: frequency curve (A), soil particle composition (B)

SP – shaddock plantation; CP – citrus plantation; GP – ginkgo plantation; RPP – *Robinia pseudoacacia* plantation; AF – abandoned farmland

https://doi.org/10.17221/84/2024-SWR

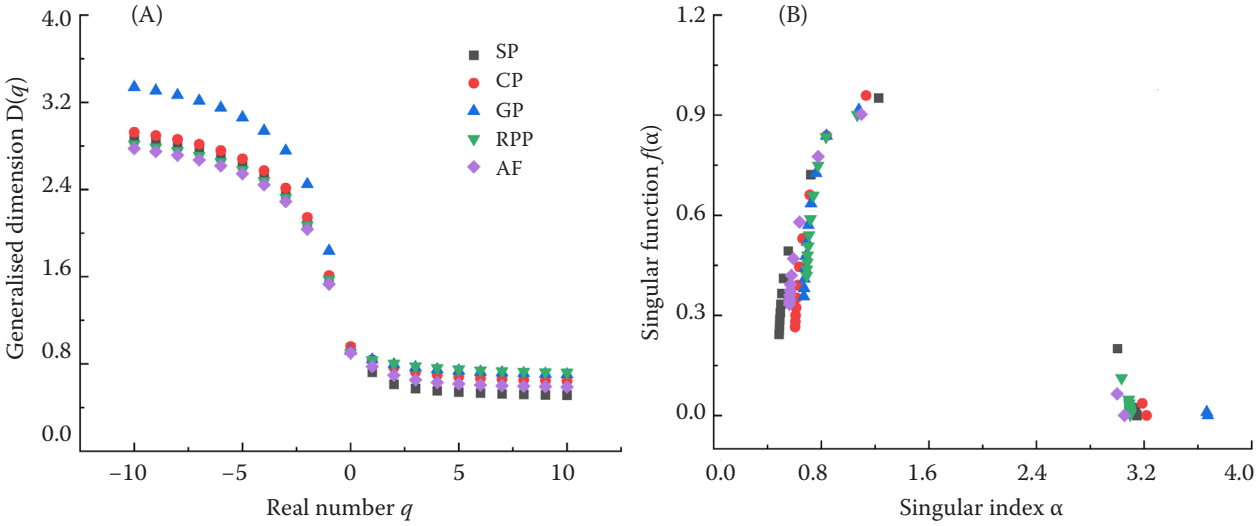

Figure 2. Generalised dimensional spectral (A) and singular spectral curves (B) of soil
SP – shaddock plantation; CP – citrus plantation; GP – ginkgo plantation; RPP – *Robinia pseudoacacia* plantation; AF – abandoned farmland

information dimension $D(1)$ and a larger $D(1)$ than correlation dimension $D(2)$ (Table 3); thus, soil PSD was anisotropic. Overall, $D(0)$ of citrus plantation was significantly higher than that of *R. pseudoacacia* plantation and abandoned farmland. $D(1)$ and $D(2)$ in citrus plantation, *R. pseudoacacia* plantation, and ginkgo plantation were significantly greater than those of shaddock plantation. $D(1)/D(0)$ values of citrus plantation, *R. pseudoacacia* plantation, ginkgo plantation, and abandoned farmland were closer to 1 and significantly greater than those of shaddock plantation. There were negligible significant differences in spectral width $\Delta\alpha$ and symmetry degree Δf of the soil singular spectrum and the single fractal dimension D between abandoned farmland and different plantations.

Characteristics of soil water repellency. No significant differences in the maximum and minimum WDPT values between the abandoned farmland and different plantations were observed (Table 4). The minimum WDPT value of *R. pseudoacacia* plantation was greater than 5 s but less than 60 s, indicating 'slight water repellency'. The minimum WDPT values of shaddock plantation, citrus plantation, ginkgo

Table 3. Fractal parameters of soil particle size distribution (PSD)

Sample plot	$D(0)$	$D(1)$	$D(2)$	$D(1)/D(0)$	$\Delta\alpha$	Δf	D
Shaddock plantation	0.95 ± 0.00^{ab}	0.72 ± 0.05^{b}	0.61 ± 0.08^{b}	0.76 ± 0.05^{b}	2.66 ± 0.68^{a}	0.24 ± 0.17^{a}	2.48 ± 0.11^{a}
Citrus plantation	0.96 ± 0.00^{a}	0.84 ± 0.03^{a}	0.77 ± 0.03^{a}	0.87 ± 0.03^{a}	2.61 ± 0.14^{a}	0.27 ± 0.13^{a}	2.74 ± 0.13^{a}
Ginkgo plantation	0.92 ± 0.04^{ab}	0.84 ± 0.05^{a}	0.80 ± 0.07^{a}	0.91 ± 0.02^{a}	3.00 ± 0.21^{a}	0.36 ± 0.05^{a}	2.66 ± 0.17^{a}
Robinia pseudoacacia plantation	0.90 ± 0.02^{b}	0.84 ± 0.00^{a}	0.80 ± 0.01^{a}	0.93 ± 0.03^{a}	2.41 ± 0.47^{a}	0.42 ± 0.12^{a}	2.71 ± 0.07^{a}
Abandoned farmland	0.90 ± 0.03^{b}	0.78 ± 0.04^{ab}	0.70 ± 0.07^{ab}	0.86 ± 0.02^{a}	2.49 ± 0.24^{a}	0.33 ± 0.13^{a}	2.59 ± 0.06^{a}

$D(0)$ – the volume dimension; $D(1)$ – the information dimension; $D(2)$ – the correlation dimension; $\Delta\alpha$ – spectral width; Δf – symmetry degree; values are mean ± standard deviation; the different lowercase letters in the same column indicated significant differences for the same variable between abandoned farmland and different plantations ($P < 0.05$)

https://doi.org/10.17221/84/2024-SWR

Table 4. Characteristics of soil water repellency

Sample plot	*W*-max	*W*-min	*W*-mean
	(s)		
Shaddock plantation	14.49 ± 11.13[a]	2.58 ± 0.52[a]	6.29 ± 3.06[b]
Citrus plantation	24.25 ± 6.72[a]	3.79 ± 1.69[a]	14.18 ± 4.53[ab]
Ginkgo plantation	28.15 ± 9.44[a]	4.60 ± 2.14[a]	17.16 ± 6.50[a]
Robinia pseudoacacia plantation	32.29 ± 5.64[a]	5.38 ± 1.68[a]	18.17 ± 3.59[a]
Abandoned farmland	23.59 ± 7.43[a]	4.75 ± 0.10[a]	14.67 ± 3.80[ab]

W-mean – average water drop penetration time; *W*-max – maximum water drop penetration time; *W*-min – minimum water drop penetration time; values in the table are mean ± standard deviation; the different lowercase letters in the same column indicated significant differences for the same variable between abandoned farmland and different plantations ($P < 0.05$)

plantation, and abandoned farmland were less than 5 s, indicating 'no water repellency'. The maximum values of WDPT were all greater than 5 s but less than 60 s, indicating 'slight water repellency'. Overall, the WDPT of *R. pseudoacacia* plantation was the highest (18.17 s), and that of the shaddock plantation was the lowest (6.29 s). Soil water repellency, in descending order, was *R. pseudoacacia* plantation > ginkgo plantation > abandoned farmland > citrus plantation > shaddock plantation, all of which indicated 'slight water repellency'. The soil water repellency of the ginkgo plantation and *R. pseudoacacia* plantation

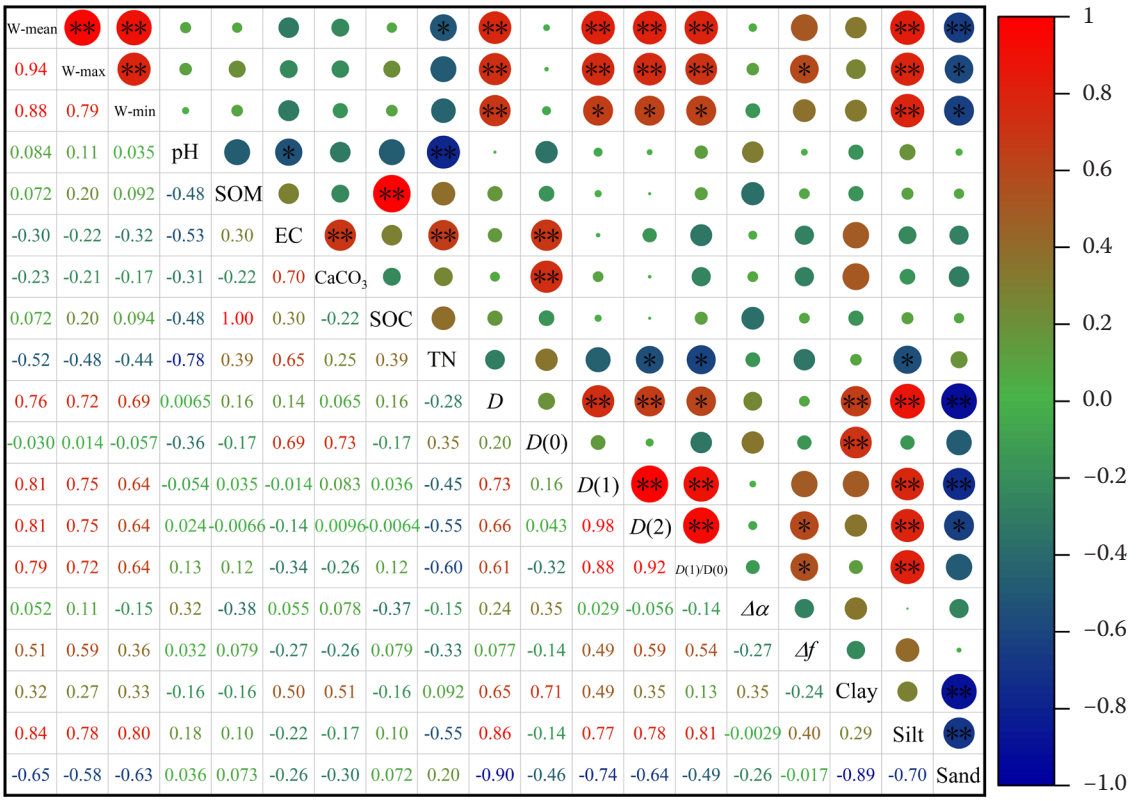

Figure 3. Correlation analysis of soil water repellency, physicochemical properties, and fractal parameters

W-mean – average water drop penetration time; *W*-max – maximum water drop penetration time; *W*-min – minimum water drop penetration time; SOM – soil organic matter; EC – electrical conductivity; SOC – soil organic carbon; TN – total nitrogen; *D*(0) – the volume dimension; *D*(1) – the information dimension; *D*(2) – the correlation dimension;Δα – spectral width; Δ*f* – symmetry degree; **, *significant correlation at 0.01 and 0.05 levels (bilateral)

https://doi.org/10.17221/84/2024-SWR

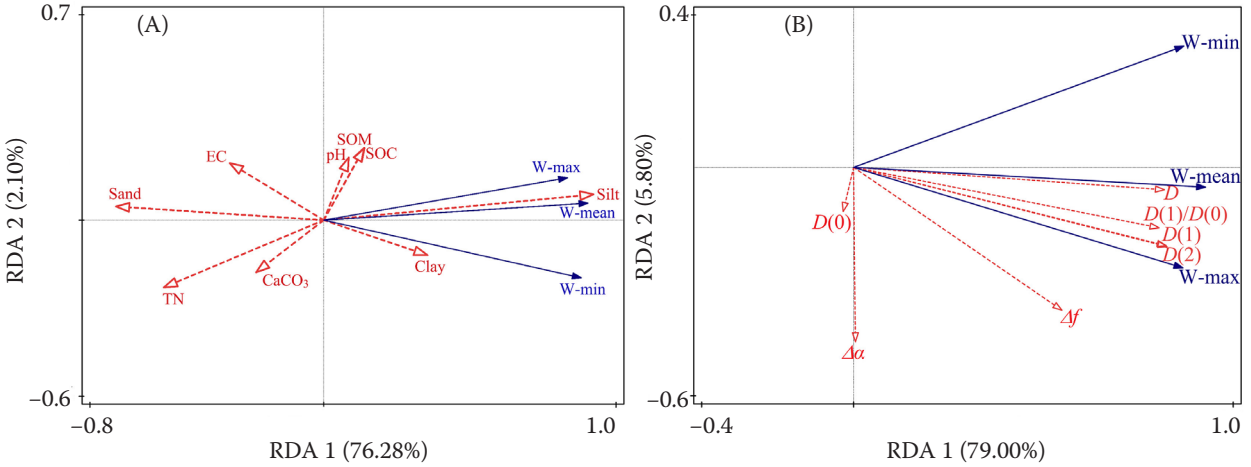

Figure 4. Redundancy analysis of the soil water repellency, physicochemical properties (A), and fractal parameters (B)
W-mean – average water drop penetration time; *W*-max – maximum water drop penetration time; *W*-min – minimum water drop penetration time; SOM – soil organic matter; SOC – soil organic carbon; TN – total nitrogen; EC – electrical conductivity; *D*(0) – the volume dimension; *D*(1) – the information dimension; *D*(2) – the correlation dimension;Δα – spectral width; Δ*f* – symmetry degree

was significantly stronger than that of the shaddock plantation.

Relationships between soil water repellency and fractal parameters. The average, maximum, and minimum values of the WDPT were significantly positively correlated with *D*, *D*(1), *D*(2), *D*(1)/*D*(0), and silt content, and significantly negatively correlated with sand content (Figure 3). The average value of the WDPT was significantly negatively correlated with TN, and the maximum value of the WDPT was significantly positively correlated with Δ*f*. The results of the redundancy analysis indicated that the first two axes of the soil physicochemical properties jointly explained 78.38% of the variation in soil water repellency, with interpretation rates of 76.28% and 2.10% for the first and second axes, respectively (Figure 4A). The first two axes of the fractal parameters jointly explained 84.80% of the variation in soil water repellency, with interpretation rates of 79.00% and 5.80% for the first and second axes, respectively (Figure 4B). These results indicated that the relationship between fractal parameters and soil water repellency was closer than the relationship between soil physicochemical properties and soil water repellency. In addition, the results of the stepwise regression demonstrated that *D*(1) independently explained 65.1% and 56.4% of the variations in the average and maximum WDPT values, respectively (Table 5). *D* alone explained 48.0% of the variation in the minimum WDPT value.

Table 5. Stepwise regression model between soil water repellency and fractal parameters

Regression model	R^2	*P*
W-mean = 80.371 × *D*(1) – 50.367	0.651	< 0.001
W-max = 124.933 × *D*(1) – 75.651	0.564	0.001
W-min = 8.235 × *D* – 17.485	0.480	0.004

W-mean – average water drop penetration time; *W*-max – maximum water drop penetration time; *W*-min – minimum water drop penetration time

DISCUSSION

Effects of vegetation types on soil particle composition and fractal parameters. The composition of soil particles is influenced by soil parent material and environmental factors, which, to some extent, can reflect the basic properties of the soil (Richer-de-Forges et al. 2022). In this study, the soil particle compositions of the abandoned farmland and different plantations were primarily sand. This result closely reflects the shallow soil layer and severe soil erosion characteristics of the karst areas (Wang et al. 2019; Li et al. 2023). The citrus plantation was well maintained manually, and the ginkgo plantation contained a large amount of surface litter. Both characteristics are beneficial for the conservation of soil moisture and the sedimentation of fine soil particles with relatively high clay content (Zhu et al. 2023). However, the soils

https://doi.org/10.17221/84/2024-SWR

of shaddock plantation, *R. pseudoacacia* plantation, and abandoned farmland are more exposed than the soils of citrus and ginkgo plantations, resulting in severe soil erosion. Some fine soil particles were washed away by rainwater, with a relatively large sand content in the soil (Qi et al. 2018).

The multifractal generalised dimension spectral function formed a reverse S-shaped monotonically declining curve. Additionally, the singular spectral function showed a rising convex left-hook curve, and $D(0) > D(1) > D(2)$. These results demonstrated that the soil PSD at all levels was non-uniform with multiple distribution characteristics of anisotropy, fulfilling the conditions of multifractal analysis (Li et al. 2022). Studies have shown that D, $D(0)$, $D(1)$, $D(2)$, $D(1)/D(0)$, Δf, and $\Delta\alpha$ can describe the characteristics of soil PSD from various perspectives (Wang et al. 2018; Li et al. 2022). Moreover, some fractal parameters exhibit the same impact when describing the characteristics of soil PSD (Li et al. 2022). In this study, the results of correlation analysis showed a close relationship among D, $D(1)$, $D(2)$, and $D(1)/D(0)$, and the correlation among Δf, $D(2)$, and $D(1)/D(0)$ was good. Thus, D, $D(1)$, $D(2)$, and $D(1)/D(0)$ can be applied to comprehensively reflect the macroscopic characteristics of soil particle composition and the concentration degree of soil PSD of abandoned farmland and different plantations. Δf, $D(2)$, and $D(1)/D(0)$ can be used to comprehensively reflect the uniformity and symmetry of soil PSD.

A significant correlation was found between the composition of soil particles and D, which is a vital factor that affects the D value (Bai et al. 2020; Li et al. 2022). Scholars have demonstrated that the larger the soil particle size, the lesser the D value, and there was a significant negative correlation between the D value and soil sand content (Bai et al. 2020; Li et al. 2022). Moreover, the D values of soils with fine texture generally range from 2.60 to 2.80, and those with coarse texture from 1.83 to 2.64 (Liu et al. 2009; Bai et al. 2020). In this study, the soil D values of citrus plantation, *R. pseudoacacia* plantation, and ginkgo plantation ranged from 2.60 to 2.80, and the soil D values of abandoned farmland and shaddock plantation ranged from 1.83 to 2.64. These results indicated that the soil texture was fine for citrus plantation, *R. pseudoacacia* plantation, and ginkgo plantation and coarse for abandoned farmland and shaddock plantation. The $D(0)$ value of citrus plantation was significantly higher than for *R. pseudoacacia* plantation and abandoned farmland, indicating a relatively wide range of soil PSD. The $D(1)$, $D(2)$, $D(1)/D(0)$ values of *R. pseudoacacia* plantation, citrus plantation, and ginkgo plantation were significantly larger than those of shaddock plantation, showing that soil PSD was more concentrated, uniform, and distributed in dense areas than in shaddock plantation. No significant differences were found in $\Delta\alpha$ and Δf between abandoned farmland and different plantations. This phenomenon may be related to the unique geological background of the karst areas. The artificial maintenance of citrus plantation and the thick litter layer of ginkgo plantation have slowed the loss of fine soil particles to certain extents; thus, sand content was considerably smaller than that of shaddock plantation, *R. pseudoacacia* plantation, and abandoned farmland (Zhu et al. 2023). However, the unique landform and lithological characteristics of karst areas cause serious water and soil losses (Peng et al. 2019). Additionally, the smaller the soil particle size, the higher the loss quality.

Factors influencing the soil water repellency. Research has shown that soil water repellency is closely related to soil physicochemical properties (Hermansen et al. 2019). The water repellent substances in soil are mainly from the decomposition of organic matter; thus, as the nutrient content in soil increases, the water repellency increases. However, in this study, the relationship between water repellency and soil nutrients was not closely related, which may be related to the types of soil nutrients (de Blas et al. 2010). Among them, soil water repellency was mainly influenced by soil free lipids and particulate organic matter (de Blas et al. 2010). Meanwhile, the results of correlation analysis indicated that the relationship between soil chemical properties and water repellency was small. Soil chemical properties were not the main reason for the difference in water repellency. The soil silt content and sand content were significantly correlated with soil water repellency, and the soil particle composition was strong different between abandoned farmland and different plantations. Therefore, in this study, soil particle composition may be the main factor affecting water repellency.

Soil particle size is a vital factor affecting soil water repellency (Qin et al. 2012). Soil particles can affect soil water repellency through the adsorption of water-repellent substances and their hydrophilic and hydrophobic properties (McHale et al. 2005). Scholars have demonstrated that with the expansion of soil particle size, soil water repellency decreases

https://doi.org/10.17221/84/2024-SWR

continuously (Qin et al. 2012). However, other researchers have demonstrated that soil water repellency decreases with a decrease in soil sand content (McKissock et al. 2002). Therefore, soil water repellency is not only related to macroscopic soil particle size but is also influenced by the local properties of soil PSD. As one of the most classical methods for studying soil particle size, applying fractal theory can explain the properties of soil PSD globally and locally (Li et al. 2022). The results of the correlation, redundancy, and stepwise regression analyses showed a significant correlation between soil water repellency and fractal parameters, and the relationship between D and $D(1)$ was the closest. The reason for this result is that the greater the values of D and $D(1)$, the greater the content of fine particles in the soil, the better the adsorption effect of water-repellent substances, the stronger their ability to fill the soil pores, and the more evident the water-repellent characteristics of the soil. Thus, fractal theory can be applied to quantitatively analyse the impact of soil PSD on soil water repellency, and fractal parameters can be used as potential indicators of the strength of soil water repellency.

CONCLUSION

This study analysed the soil particle size distribution and water repellency of abandoned farmland and different plantations in karst areas. The results indicated that sand content in shaddock plantation and clay content in citrus plantation was the highest. The soil particles of abandoned farmland and plantations were primarily sand. The values of volume dimension $D(0)$ in descending order were citrus plantation, shaddock plantation, ginkgo plantation, *R. pseudoacacia* plantation, and abandoned farmland. The values of information dimension $D(1)$, correlation dimension $D(2)$, and information dimension/volume dimension $D(1)/D(0)$ in descending order were *R. pseudoacacia* plantation, ginkgo plantation, citrus plantation, abandoned farmland, and shaddock plantation. No significant differences were found in the symmetry degree Δf, the spectral width $\Delta\alpha$ of the singular spectral function, and the single fractal dimension D among the abandoned farmland and different plantations. The degree of water repellency in descending order was *R. pseudoacacia* plantation > ginkgo plantation > abandoned farmland > citrus plantation > shaddock plantation. There was a significant correlation between the fractal parameters and water repellency, and fractal parameters were suitable potential indicators for soil water repellency.

Acknowledgements. The authors would like to thank the editors and anonymous reviewers for their comments and suggestions which greatly helped us to improve this manuscript.

REFERENCES

Abou Najm M.R., Stewart R.D., Di Prima S., Lassabatere L. (2021): A simple correction term to model infiltration in water-repellent soils. Water Resources Research, 57: e2020WR028539.

Bai Y., Qin Y., Lu X., Zhang J., Chen G., Li X. (2020): Fractal dimension of particle-size distribution and their relationships with alkalinity properties of soils in the western Songnen Plain, China. Scientific Reports, 10: 20603.

Banfield C.C., Braun A.C., Barra R., Castillo A., Vogt J. (2018): Erosion proxies in an exotic tree plantation question the appropriate land use in Central Chile. Catena, 161: 77–84.

Buczko U., Bens O., Hüttl R.F. (2005): Variability of soil water repellency in sandy forest soils with different stand structure under Scots pine (*Pinus sylvestris*) and beech (*Fagus sylvatica*). Geoderma, 126: 317–336.

Carter M.R. (2004): Researching structural complexity in agricultural soils. Soil and Tillage Research, 79: 1–6.

Chen J., McGuire K.J., Stewart R.D. (2020): Effect of soil water-repellent layer depth on post-wildfire hydrological processes. Hydrological Processes, 34: 270–283.

de Blas E., Rodríguez-Alleres M., Almendros G. (2010): Speciation of lipid and humic fractions in soils under pine and eucalyptus forest in northwest Spain and its effect on water repellency. Geoderma, 155: 242–248.

Deng Y., Wang S., Bai X., Luo G., Wu L., Chen F., Wang J., Li Q., Li C., Yang Y., Hu Z., Tian S. (2020): Spatiotemporal dynamics of soil moisture in the karst areas of China based on reanalysis and observations data. Journal of Hydrology, 585: 124744.

Doerr S.H., Thomas A.D. (2000): The role of soil moisture in controlling water repellency: new evidence from forest soils in Portugal. Journal of Hydrology, 231–232: 134–147.

Doerr S.H., Shakesby R.A., Walsh R.P.D. (2000): Soil water repellency: Its causes, characteristics and hydrogeomorphological significance. Earth-Science Reviews, 51: 33–65.

Duan W.J., Ren H., Fu S.L., Wang J., Zhang J.P., Yang L., Huang C. (2010): Community comparison and determi-

https://doi.org/10.17221/84/2024-SWR

nant analysis of understory vegetation in six plantations in South China. Restoration Ecology, 18: 206–214.

Gao Z., Niu F., Lin Z., Luo J. (2021): Fractal and multifractal analysis of soil particle-size distribution and correlation with soil hydrological properties in active layer of Qinghai-Tibet Plateau, China. Catena, 203: 105373.

Hermansen C., Moldrup P., Müller K., Jensen P. W., van den Dijssel C., Jeyakumar P., de Jonge L.W. (2019): Organic carbon content controls the severity of water repellency and the critical moisture level across New Zealand pasture soils. Geoderma, 338: 281–290.

Jordan A., Zavala L.M., Mataix-Solera J., Doerr S.H. (2013): Soil water repellency: Origin, assessment and geomorphological consequences. Catena, 108: 1–5.

Ke Z., Ma L., Jiao F., Liu X., Liu Z., Wang Z. (2021): Multifractal parameters of soil particle size as key indicators of the soil moisture distribution. Journal of Hydrology, 595: 125988.

Li J., Bao Y., Wei J., He X., Tang Q., Wu S., Huang P., Ma M., Zhou P., Wang M. (2022): Scaling properties of particle-size distributions of purple soils in a small agricultural watershed: A multifractal analysis. Catena, 215: 106326.

Li R., Gao J., He M., Jing J., Xiong L., Chen M., Zhao L. (2023): Effect of rock exposure on runoff and sediment on karst slopes under erosive rainfall conditions. Journal of Hydrology: Regional Studies, 50: 101525.

Liu X., Zhang G., Heathman G.C., Wang Y., Huang C. (2009): Fractal features of soil particle-size distribution as affected by plant communities in the forested region of Mountain Yimeng, China. Geoderma, 154: 123–130.

McHale G., Newton M.I., Shirtcliffe N.J. (2005): Water-repellent soil and its relationship to granularity, surface roughness and hydrophobicity: a materials science view. European Journal of Soil Science, 56: 445–452.

McKissock I., Gilkes R.J., Walker E.L. (2002): The reduction of water repellency by added clay is influenced by clay and soil properties. Applied Clay Science, 20: 225–241.

Nunes J.P., Malvar M., Benali A.A., Rivas M.E.R., Keizer J.J. (2016): A simple water balance model adapted for soil water repellency: Application on Portuguese burned and unburned eucalypt stands. Hydrological Processes, 30: 463–478.

Pang D.B., Cao J.H., Dan X.Q., Guan Y.H., Peng X.W., Cui M., Wu X.Q., Zhou J.X. (2018): Recovery approach affects soil quality in fragile karst ecosystems of southwest China: Implications for vegetation restoration. Ecological Engineering, 123: 151–160.

Peng X., Dai Q., Ding G., Li C. (2019): Role of underground leakage in soil, water and nutrient loss from a rock-mantled slope in the karst rocky desertification area. Journal of Hydrology, 578: 124086.

Piyaruwan H.I.G.S., Leelamanie D.A.L. (2020): Existence of water repellency and its relation to structural stability of soils in a tropical Eucalyptus plantation forest. Geoderma, 380: 114679.

Qi F., Zhang R., Liu X., Niu Y., Zhang H., Li H., Li J., Wang B., Zhang G. (2018): Soil particle size distribution characteristics of different land-use types in the Funiu mountainous region. Soil and Tillage Research, 184: 45–51.

Qin J., Zhao L., Sun H., Li S. (2012): Preliminary study on the characteristics of soil repellency in the dry valley of Minjiang River. Journal of Soil and Water Conservation, 26: 259–262. (in Chinese)

Richer-de-Forges A.C., Arrouays D., Chen S., Dobarco M.R., Libohova Z., Roudier P., Minasny B., Bourennane H. (2022): Hand-feel soil texture and particle-size distribution in central France. Relationships and implications. Catena, 213: 106155.

Roper M.M., Ward P.R., Keulen A.F., Hill J.R. (2013): Under no-tillage and stubble retention, soil water content and crop growth are poorly related to soil water repellency. Soil and Tillage Research, 126: 143–150.

Smettem K.R.J., Rye C., Henry D.J., Sochacki S.J., Harper R.J. (2021): Soil water repellency and the five spheres of influence: A review of mechanisms, measurement and ecological implications. Science of the Total Environment, 787: 147429.

Sun Q., Liu Q., Yu X., Li J., Zeng Z. (2014): Spatial response of water repellency to physicochemical properties in peach (*Prunuspersica*) orchard brown soil in Yimeng mountains. Acta Pedologica Sinica, 51: 648–655. (in Chinese)

Tian Y., Wang S., Bai X., Luo G., Xu Y. (2016): Trade-offs among ecosystem services in a typical Karst watershed, SW China. Science of the Total Environment, 566: 1297–1308.

Tian Z., Pan Y., Chen M., Zhang S., Chen Y. (2023): The relationships between fractal parameters of soil particle size and heavy-metal content on alluvial-proluvial fan. Journal of Contaminant Hydrology, 254: 104140.

Vogelmann E.S., Reichert J.M., Prevedello J., Awe G.O., Cerda A. (2017): Soil moisture influences sorptivity and water repellency of topsoil aggregates in native grasslands. Geoderma, 305: 374–381.

Wang J., Zhang M., Bai Z., Guo L. (2015): Multi-fractal characteristics of the particle distribution of reconstructed soils and the relationship between soil properties and multi-fractal parameters in an opencast coal-mine dump in a loess area. Environmental Earth Sciences, 73: 4749–4762.

Wang J., Lu X., Feng Y., Yang R. (2018): Integrating multifractal theory and geo-statistics method to character-

https://doi.org/10.17221/84/2024-SWR

ize the spatial variability of particle size distribution of minesoils. Geoderma, 317: 39–46.

Wang K., Zhang C., Chen H., Yue Y., Zhang W., Zhang M., Qi X., Fu Z. (2019): Karst landscapes of China: Patterns, ecosystem processes and services. Landscape Ecology, 34: 2743–2763.

Wang X., Sun L., Zhao N., Li W., Wei X., Niu B. (2022a): Multifractal dimensions of soil particle size distribution reveal the erodibility and fertility of alpine grassland soils in the Northern Tibet Plateau. Journal of Environmental Management, 315: 115145.

Wang Y., He Y., Zhan J., Li Z. (2022b): Identification of soil particle size distribution in different sedimentary environments at river basin scale by fractal dimension. Scientific Reports, 12: 10960.

Xu X.L., Ma K.M., Fu B.J., Liu W., Song C.J. (2009): Soil and water erosion under different plant species in a semiarid river valley, SW China: The effects of plant morphology. Ecological Research, 24: 37–46.

Yi R., Xu X., Zhu S., Zhang Y., Zhong F., Zeng X., Xu C. (2021): Difference in hydraulic resistance between planted forest and naturally regenerated forest and its implications for ecosystem restoration in subtropical karst landscapes. Journal of Hydrology, 596: 126093.

Zhang H., Luo Y., Makino T., Wu L., Nanzyo M. (2013): The heavy metal partition in size-fractions of the fine particles in agricultural soils contaminated by waste water and smelter dust. Journal of Hazardous Materials, 248: 303–312.

Zhu D., Yang Q., Zhao Y., Cao Z., Han Y., Li R., Ni J., Wu Z. (2023): Afforestation influences soil aggregate stability by regulating aggregate transformation in karst rocky desertification areas. Forests, 14: 1356.

Received: July 18, 2024
Accepted: February 3, 2025
Published online: February 11, 2025